熱帶大西洋對夏季西北太平洋副熱帶高壓的影響

張道奇[1]　許晃雄[1]　洪志誠[2]

[1] 中央研究院環境變遷研究中心

[2] 臺北市立教育大學地球環境暨生物資源學系

關鍵字：西太平洋副熱帶高壓，熱帶大西洋，年際變化，海表面溫度

Influence of the Tropical Atlantic on the Western North Pacific Subtropical High in the boreal summer

Tao-Chi Chang[1], and Huang-Hsiung Hsu[1], Chi-Cherng Hong[2],

[1]Research Center for Environmental Changes, Academia Sinica, Taipei, Taiwan,

[2]Department of Earth and Life, University of Taipei, Taipei, Taiwan

Abstract

Sea surface temperature (SST) is one of the important factors that affect the Western North Pacific subtropical high (WNPSH). The interannual correlation between the WNPSH and SST in the Tropical Atlantic (TA) dramatically increased after the early 1980s, suggesting an enhanced influence of TA SST. In this study, we provide various evidences to demonstrate this enhanced influence of TA SST by empirical diagnostics and numerical modeling. Singular Value Decomposition (SVD) analysis reveals the emergence of a quadrupole circulation pattern that prevails from the boreal spring to summer and results in weaker monsoon flow and warming in the Northern Indian Ocean (NIO). This feature later becomes a part of the WNP-NIO coupling system proposed by Wang et al. (2013) and has an effect in enhancing the WNPSH. This hypothesis is verified in a serious of numerical simulations using a simplified atmospheric general circulation model coupled with a slab ocean model.

Key words: Western North Pacific subtropical high, Tropical Atlantic, interannual variability, sea surface temperature

I. Introduction

The Western North Pacific Subtropical High (WNPSH) is one of the dominant factors that control the Eastern Asian climate and weather systems in the boreal summer. Several studies suggested the import influence of sea surface temperature (SST) in various ocean basins, such as the Northern Indian Ocean (NIO), the Maritime Continent (MC), and the Western North Pacific (WNP) [e.g., Xie et al. (2009, 2010); Wu et al. (2010); Chung et al. (2011)]. Intensification of these influences near the early 1980s was also suggested. Wang et al. (2013) has integrated some of those theories by the first leading component of the summer WNPSH, proposing a WNP-NIO coupling system, a positive feedback system between the NIO and the WNP.

In this study, we demonstrate the influence of the Tropical Atlantic (TA), which was seldom mentioned before. Ham et al. (2013) suggested that there is a teleconnection existing between the Northern TA and tropical Pacific atmospheric anomalies. Hong et al. (2014) analyzed the variability of the WNPSH and its relationships with the global SST, finding that there is strong linkage at interannual time scale between the WNPSH and the TA SST after the early 1980s, with SST distribution covering the northern TA.

Exploring the causality between them is the main purpose of this study. We apply regression and partial correlation analysis to confirm the influences of the TA SST and construct a regression relationship to show the ability of the TA SST to reconstruct the WNPSH starting from spring and to bypass the spring barrier problem in seasonal prediction. Finally, based on singular value decomposition (SVD) analysis and numerical experiments, we demonstrate how the TA SST affects the SST in the Indian Ocean and contribute to the WNP-NIO coupling system after the early 1980s.

II. Data, Methods, and Model

1. Data

Several datasets are used in this study: 1) monthly atmospheric data from National Centers for Environmental Prediction/National Center for Atmospheric Re-search (NCEP/NCAR) Reanalysis I [Kalnay et al. (1996)], 2) monthly oceanic data from NOAA Extended Reconstructed SST v3b (ERSST v3b) [Smith et al. (2008)], 3) monthly rainfall data from Global Precipitation Climatology Project (GPCP) version 2.2 [Adler et al. (2003)], and 4) tropical cyclone track data from International Best Track Archive for Climate Stewardship (IBTrACS) v03r05 [Schreck III et al. (2014)].

Following Hong et al. (2014), the WNPSH index is defined as the 850 hPa streamfunction averaged over (15°–25°N, 130°–150°E) where variance is maximum in summer. TA, NIO and ECP SST indices are defined as the SST averaged over (0–20°N, 25°–80°W), (0–20°N, 50°–100°E), and (-5°S–5°N, 170°–240°E), respectively. Nine-year running means and the long-term linear trends were removed to isolate the interannual variability. The analyzed period is separated into two epochs, 1948-1980 and 1981-2012.

2. Methodology

Two methods are used in this study: Partial Correlation and Singular Value Decomposition (SVD).

Partial correlation is a method used to calculate the residual correlation showing what would have happened if the influence of one or some particular variables had been removed. SVD is a method to identify a series of paired variability modes between two variables based on the ranking of the squared covariance fractions (SCFs).

3. Model

The model used is the ICTP AGCM version 41, an atmospheric general circulation model (AGCM) developed at the Abdus Salam International Centre for Theoretical Physics (ICTP), also called “SPEEDY” (Simplified Parameterizations, primitivE-Equation Dynamics) [Kucharski et al., 2013]. This model is a model of intermediate complexity, which can be forced by monthly SST anomaly (SSTA) and/or through coupling with a slab ocean model. This model has eight vertical levels with T30 horizontal resolution.

III. Empirical diagnostics

1. Decadal shift and Relationships

Fig. 1 shows the amplitude envelope function (AEF) of the WNPSH index calculated from three datasets. Regime shift test [Rodionov and Overland (2005)] indicates a significant shift near 1981 in all three datasets, so does the AEF of the TA index shown in Fig. 2(a). This shift is also evident by seeing the enhanced relationship between the WNPSH index and the 850hPa stream function in WNP and the SST in the NIO in the later epoch.

The significant relationship between the TA SST and the WNPSH in the later epoch also appears in the composites of precipitation and tropical cyclone (TC) track density (Fig. 3). Warmer TA SST and stronger WNPSH resulted in the less precipitation and lower TC track density.

2. Influence from Tropical Atlantic

In order to exclude the influences of the factors other than TA SST, such as NIO and ECP SST, two approaches are taken.

One is partial correlation shown in Fig. 4, in which we remove the NIO and ECP indices simultaneously and individually. The residual correlation in Fig. 4d clearly shows the influence of TA SST after removing the effects of NIO and ECP SST.

The other is the regression function based on three SST indices:

$$WNPSH_{obs} = \beta_{TA} \times SST_{TA} + \beta_{ECP} \times SST_{ECP} + \beta_{NIO} \times SST_{NIO} + \beta_0$$

$$WNPSH' = \beta_i \times SST_i + \beta_0 .$$

Correlation coefficients between the $WNPSH_{obs}$ and WNPSH' in earlier and later epochs presented in Fig. 5 mark the season when the influence of various SST begins. The influence of TA SST on the WNPSH becomes much more significant after spring and only in the later epoch, while the influences of NIO and ECP SST remain similar in both epochs.

3. SVD analysis

SVD analysis provides us a way to obtain the co-variability modes associated with the TA SST, NIO SST, and WNPSH. The second leading mode (Fig. 6b) is the particular mode we are looking for: warm SST in the TA and NIO and a quadrupole structure of low-level circulation. Also, the time series is highly correlated with the TA index especially in the later epoch (Fig. 6c).

We also apply calculate partial correlation maps with 850hPa velocity potential and stream function based onSVD2 time series. Correlation maps presented in Fig. 7a and 7b show the development of the quadrupole pattern and associated velocity potential from March/April, May/June, to July/August. Similar evolution is examined by removing the effect of NIO and ECP SST. Fig. 7c and 7d show that the Walker circulation and the quadrupole structure are weakened in MJ and JA when the TA index is removed. On the other hand, Fig. 7e and 7f show that even when the NIO and ECP indices are removed, the correlations associated with the TA SST alone is still evident in JA.

Fig. 8 examines the local mechanism. In the SVD2, warm NIO SST corresponds to anomalous easterlies and net heat fluxes into the ocean, resembling the WNP-NIO coupling system proposed by Wang et al. (2013). When the effect of the TA index is removed, the negative correlations weaken in summer (Fig. 9), implying a weaker easterly anomaly and suggesting the effect of the warm TA SST on the NIO SSTA.

IV. Simulations

1. Experiment setting

In order to confirm our hypothesis, we conducted three 100-year experiments (1911 to 2010), each with five members. In Exp_TA, the observed monthly SSTA is prescribed only in the TA region (Fig. 10a), while observed climatological monthly SST is prescribed in other ocean basins. In Exp_cup, we turned on the air-sea interaction in the tropical Pacific and the TIO (Fig. 10b) but without prescribing TA SSTA. The Exp_cupTA is a simulation with prescribed SSTA in TA and air-sea interaction turned on in the tropical Pacific and the TIO.

2. Results

The SVD results of the simulated results are shown in Fig. 11. Comparing the SVD1 of the Exp_cupTA (Fig. 11a) to the observational SVD2, we recognize a quadrupole circulation structure over the Pacific and SST pattern similar to the observation. When the air-sea interaction is turned off, in the SVD1 of Exp_TA (Fig. 11b), the effect resulted from the TA SSTA is emphasized so that the anomalously cyclonic circulation pair over the EP is simulated and extends to the western Pacific. In the Exp_cup with no the TA SST forcing and only air-sea interaction functioning (Fig. 11c), an anticyclonic pair is simulated, with a weak positive in the WNP) and weak warm SST in the NIO. A comparison among three experiments suggests that the atmospheric response induced by the TA SSTA enhances through the air-sea interaction.

The lag correlations of the large-scale circulations (Fig. 12) show that without air-ocean interaction, the effect of the TA SSTA overreact as a westward shift of convection. The air-ocean interaction evidently functions as a buffer, providing a balance to the influence of the TA SSTA.

To verify the hypothesis about easterlies and the WNP-NIO coupling system, we compare the regression of wind anomalies and net heat flux (Fig. 13) to the observation. In Exp_TA, the strong easterlies happen in MJ and obviously overreact in JA. If the air-ocean interaction is involved, the response to the TA SSTA forcing is reduced and the result of Exp_cupTA becomes more similar to the observation.

V. Summary

After the early 1980s, enhanced relationship between the TA SST and several climate systems in the WNP and IO regions in summer at the interannual time scale is observed. The empirical diagnostics show that in JA as long as the TA SST is warmer, there are higher SST in the NIO, stronger anticyclone in the WNP (WNPSH), less WNP precipitation, and the lower tropical cyclone density in the WNP.

Partial correlations and regression functions illustrate that the sole influence of the TA SST on the WNPSH exists and becomes significant after spring. Results of SVD analysis suggests the influence of TA SST on the quadruple circulation pattern that implying the enhancement of the WNP-NIO coupling system that strongly influence the WNPSH in summer.

Numerical simulations confirm that both the TA SSTA forcing and the air-ocean interaction are essential to intensify the WNPSH. The TA SSTA forcing can excite a Walker circulation from the eastern Pacific to the western, and drive stronger easterlies in the NIO. The WNP-NIO coupling mechanism is enhanced through air-sea interaction and results in stronger influence on the WNPSH.

In our study, details about the influence process, such as tropical cyclone tracks, the surface wind, and the NIO SST are discussed. We expect that the seasonal or interannual predictability of not only the WNPSH but also other relevant phenomena can be improved by involving the TA SST.

VI. References

Adler, R. F. et al. The Version-2 Global Precipitation Climatology Project (GPCP) Monthly Precipitation Analysis (1979–Present). J. Hydrometeorol. 4, 1147–1167 (2003).

Chung, P. P.-H., Sui, C.-H. & Li, T. Interannual relationships between the tropical sea surface temperature and summertime subtropical anticyclone over the western North Pacific. J. Geophys. Res. 116, 1–19 (2011).

Ham, Y. G., Kug, J. S. & Park, J. Y. Two distinct roles of Atlantic SSTs in ENSO variability: North Tropical Atlantic SST and Atlantic Ni??o. Geophys. Res. Lett. 40, 4012–4017 (2013).

Hong, C.-C., Chang, T.-C. & Hsu, H.-H. Enhanced Relationship between the Tropical Atlantic SST and the Summertime Western North Pacific Subtropical High after the early 1980s. J. Geophys. Res. Atmos.(2014). doi:10.1002/2013JD021394

Kalnay, E. et al. The NCEP/NCAR 40-Year Reanalysis Project. Bull. Am. Meteorol. Soc. 77, 437–471 (1996).

Kucharski, F. et al. On the Need of Intermediate Complexity General Circulation Models: A ‘SPEEDY’ Example. Bull. Am. Meteorol. Soc. 94, 25–30 (2013).

Rodionov, S., & Overland, J. E. (2005). Application of a sequential regime shift detection method to the Bering Sea ecosystem. *ICES Journal of Marine Science*, *62*(3), 328–332. http://doi.org/10.1016/j.icesjms.2005.01.013

Schreck, C. J., Knapp, K. R. & Kossin, J. P. The Impact of Best Track Discrepancies on Global Tropical Cyclone Climatologies using IBTrACS. Mon. Weather Rev. 142, 3881–3899 (2014).

Smith, T. M., Reynolds, R. W., Peterson, T. C. & Lawrimore, J. Improvements to NOAA’s historical merged land-ocean surface temperature analysis (1880-2006). J. Clim. 21, 2283–2296 (2008).

Wang, B., Xiang, B. & Lee, J.-Y. Subtropical high predictability establishes a promising way for monsoon and tropical storm predictions. Proc. Natl. Acad. Sci. U. S. A. 110, 2718–22 (2013).

Xie, S.-P. et al. Indian Ocean Capacitor Effect on Indo–Western Pacific Climate during the Summer following El Niño. J. Clim. 22, 730–747 (2009).

Xie, S.-P. et al. Decadal Shift in El Niño Influences on Indo–Western Pacific and East Asian Climate in the 1970s*. J. Clim. 23, 3352–3368 (2010).

VII. Figures

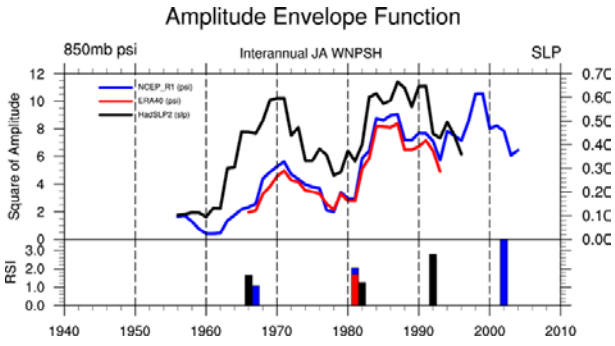

Fig. 1 The amplitude envelope function (AEF) of the WNPSH indices made from different data set, made from the 9-year running mean of the square of each indices. The bottom is the regime shift index, showing the level of the decadal shift.

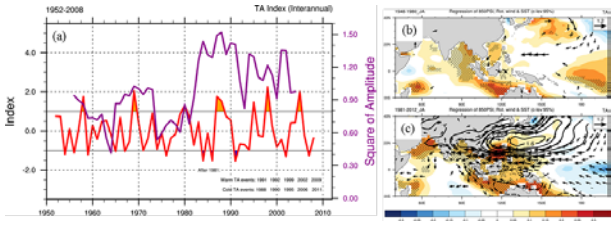

Fig. 2 (a) The TA index (red) and its AEF (purple) TA index. The warm and cold TA events are classified by the first standard deviations, and those in the later epoch are shown in the bottom. Regressions of the SST (shading), stream function (contour), and rotational winds at 850 hPa on the TA index in (b) the earlier and (c) the later epoch. The vectors, the contours, and the dots in shading are shown if exceeding the 95% significant level.

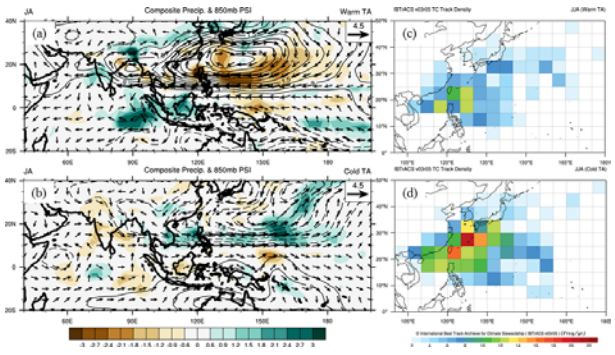

Fig. 3 (a) The warm-TA and (b) cold-TA composites of the precipitation (shading), 850 hPa stream function (contour), and rotational winds. The warm and cold years defined in Fig. 2a are used. (c) The warm-TA and (d) cold-TA composites of tropical cyclone (TC) track density.

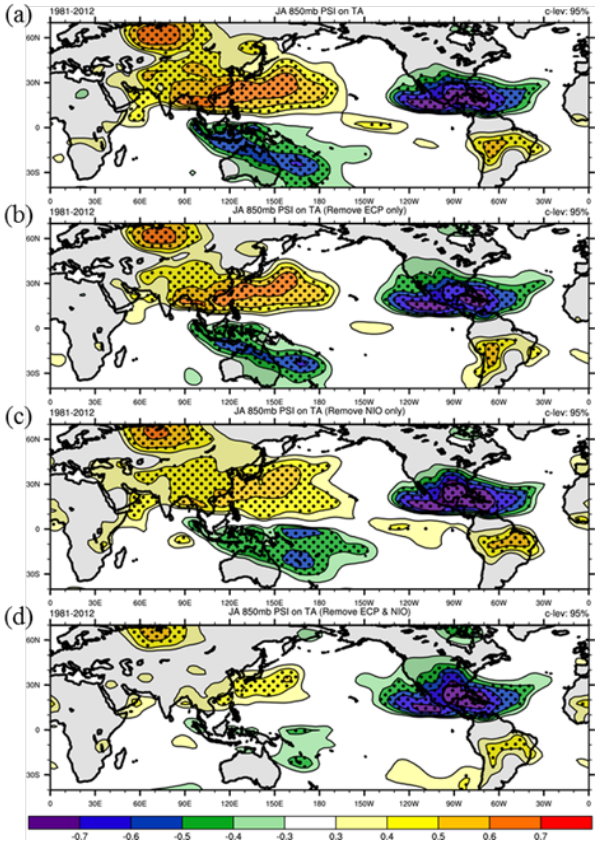

Fig. 4 (a) Correlation coefficients between the 850 hPa stream function and the TA index in the later epoch. The dots in shading represent the values exceeding the 95% significant level. Partial correlation coefficients without the influences of the (b) ECP and (c) NIO SSTs in JA respectively. (d) As (b), but removing both the ECP and NIO index.

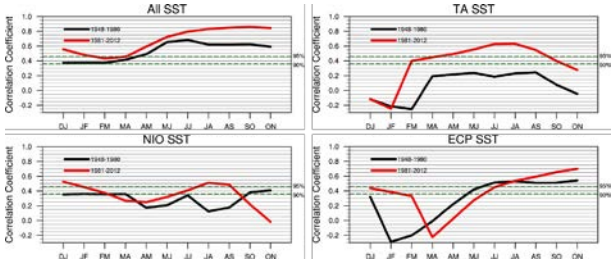

Fig. 5 The monthly correlation coefficients between the observational WNPSH index and the reconstructed WNPSH index in earlier (black) and later (red) epochs.

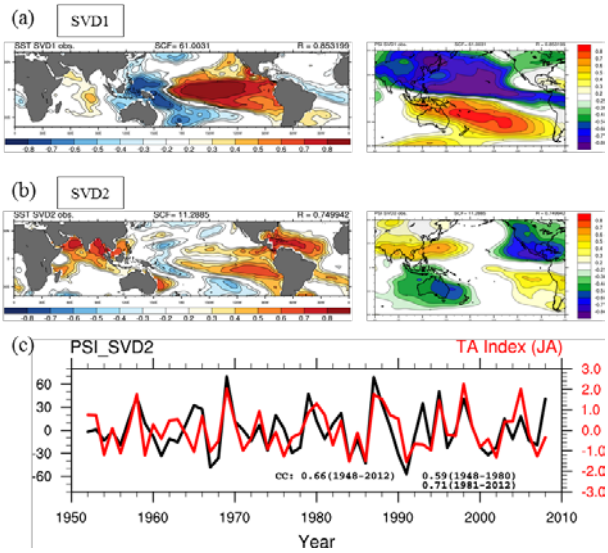

Fig. 6 (a) The first leading mode of the observational SVD analysis with the SST part (left) and the 850 hPa stream function part (right) (b) As (a), the second leading mode. (c) TA index (red), the time series of the stream function part of the SVD2 (block), and the correlation coefficients between them in different epochs shown below.

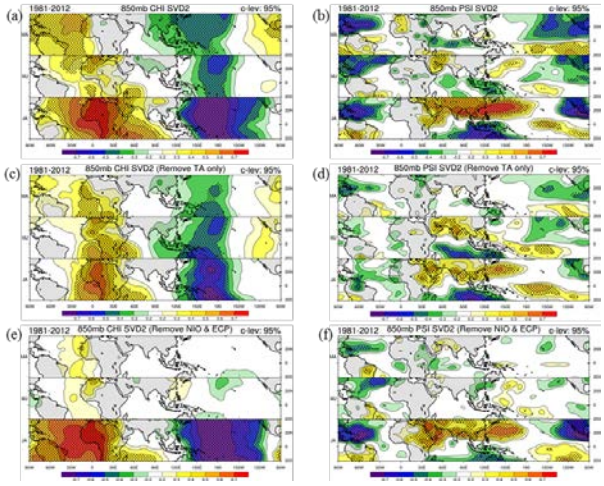

Fig. 7 Regular correlation patterns of the 850 hPa (a) velocity potential and (b) stream function with the observational SVD2. In (c) and (d), the influence of the TA index is removed from (a) and (b). In (e) and (f), as in (c) and (d), but without the influences of both the NIO and ECP SST. The dots in shading are shown if exceeding the 95% significant level.

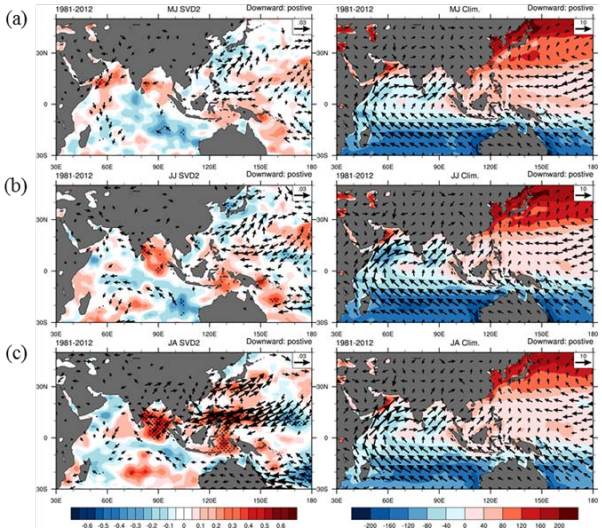

Fig. 8 Regressions on the observational SVD2 (left panel) and the climatological patterns (right panel) of the net heat fluxes into the ocean (shading) and 10 meter winds in the (a) MJ, (b) JJ, and (c) JA. The net heat flux is defined as the sum of the net long wave radiation, net short wave radiation, latent heat flux, and sensible heat flux. The vectors and the dots in shading are shown if exceeding the 95% significant level.

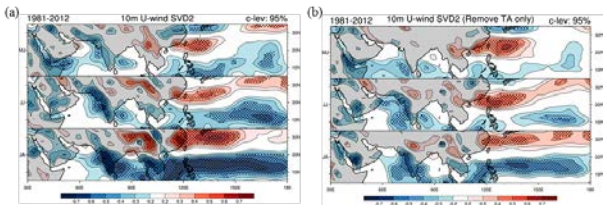

Fig. 9 (a) The regular lag correlation of the 10 meter winds on the observational SVD2 from the MJ to JA. (b) As (a), except for the partial correlations where the TA index is removed. The dots in shading are shown if exceeding the 95% significant level.

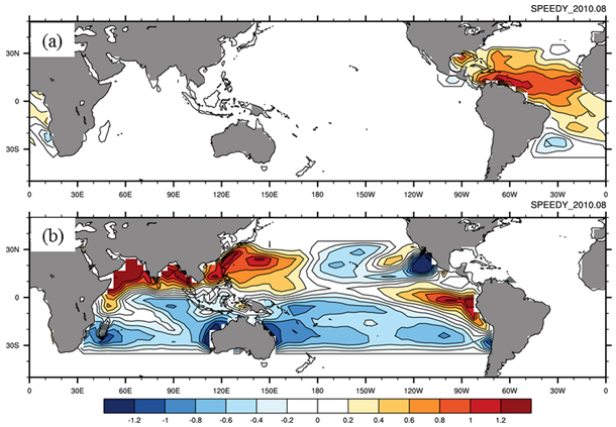

Fig. 10 (a) The area of the TA SSTA forcing used in the experiments. We take the SSTA of an arbitrary month (August 2010) as an example. (b) As (a), but for the area where the air-ocean interaction is turned on.

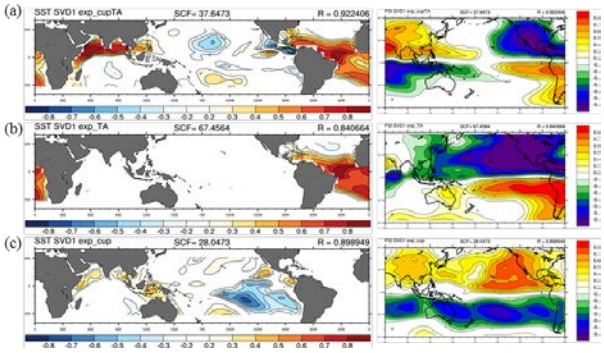

Fig. 11 (a) The SST (left) and the 850 hPa stream function (right) patterns of the first lead mode in the SVD analysis of Exp_cupTA. As (a), but for the results of (b) Exp_TA and (c) Exp_cup.

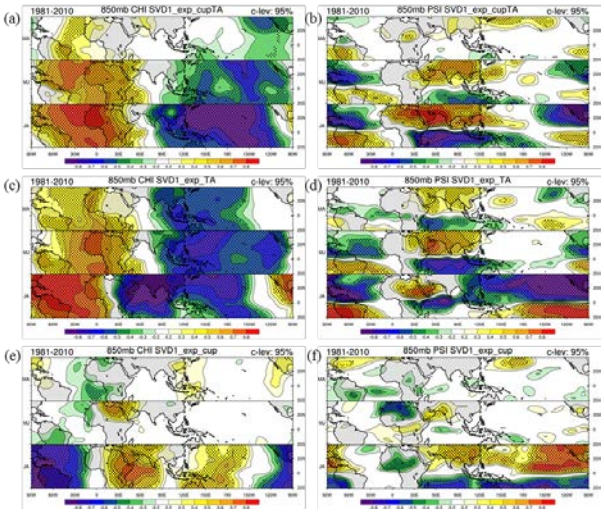

Fig. 12 Lag correlation as Fig. 7a and 7b, except for using the experimental results of Exp_cupTA in (a) and (b). Similarly, we use the results of Exp_TA in (c) and (d) and the results of Exp_cup in (e) and (f).

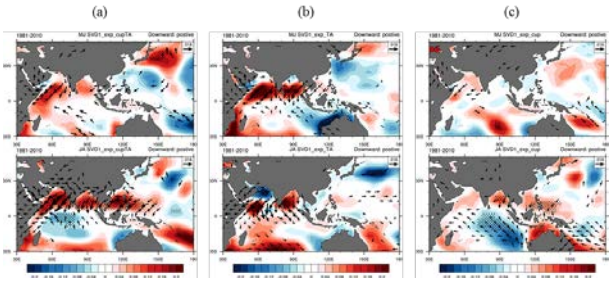

Fig. 13 (a) Lag regression of the surface winds and net heat flux into the ocean on the SVD1 of Exp_cupTA in the MJ and JA. As (a), but for (b) Exp_TA and (c) Exp_cup. The vectors and the dots in shading are shown if exceeding the 95% significant level.